Lattice deformation on flat-band modulation in 3D Hopf-linked carbon allotrope: Hopfene

Isao Tomita*
Sustainable Electronic Technologies, Electronics and Computer Science, Faculty of Physical Sciences and Engineering, University of Southampton, SO17 1BJ, UK and Department of Electrical and Computer Engineering, National Institute of Technology, Gifu College, Gifu 501-0495, Japan

Shinichi Saito
Sustainable Electronic Technologies, Electronics and Computer Science, Faculty of Physical Sciences and Engineering, University of Southampton, SO17 1BJ, UK

(Dated: July 10, 2019)

Flat bands form in a 3D Hopf-linked graphene crystal or a 3D carbon allotrope named Hopfene, which qualitatively differ from bands of only graphenes. This paper discusses carbon-hexagon deformation on the level shift of a flat band via density-functional-theoretical (DFT) analysis to set the flat-band level to the Fermi level, viz., to utilize its large density of states for magnetic- and electronic-property researches. Tight-binding (TB) analysis is also performed for a comparison with the DFT analysis; here, a qualitative agreement between TB and DFT bands is obtained. The DFT analysis shows an almost linear flat-band level shift to the lattice-deformation rate, where electron-interaction effects are included within the Kohn-Sham method. To tune the flat-band level so that it fits the Fermi level, a double-hetero-like structure is also proposed as a way of hexagon-deformation control.

Carbon allotropes that have been found for the past three decades, such as fullerenes [1], nanotubes [2], and graphenes [3], have uncovered that *morphology* (even though the material is the same) greatly changes the fundamental mechanical, electrical, and optical properties of the material [4–7]. These opened very useful device and material applications in nano-electronics and material science, and also developed basic physics researches related to Tomonaga-Luttinger liquid [8], superconductivity [9], quantum Hall effect [10], and Kosterlitz-Thouless transition [11]. The ground-breaking discovery of fullerenes and graphenes, linked to those advanced fundamental and applied researches, won Nobel prizes in 1996 and 2010, respectively.

Morphology, including topological one, has now been attracting a great deal of attention not only in physics dealing with the above allotropes and related researches but also in chemistry treating artificially-designed molecules that can be used as molecular machines [12]; the latter also won Nobel prize in 2016. As for carbon structures, we have recently developed other types of allotropes from a topological point of view [13]. In a crystal-type topological allotrope among them, named *Hopfene* (see Fig. 1(a)), we have revealed some unusual electronic properties by band-structure analyses [14], and also have found striking 3D-Dirac/Weyl-fermionic features [15]. Here, the terminology *Hopfene* originates from a crystal with *Hopf*-linked intersections, named after topologist Heinz Hopf who studied these links greatly.

Until now we have shown structural sustainability of Hopfenes via semi-empirical molecular-orbital [13] and density-fractional-theoretical (DFT) [14, 16, 17] methods (although the graphene-sheet insertion parallel to the x-z plane (the y-z plane) swells the carbon hexagons in the y direction (x direction), as depicted in Figs. 1(b)(c)). In this paper, we examine this hexagon swelling on the band structure, particularly on flat bands, via DFT analysis. Before doing this by heavy numerical computations, we carry out simple tight-binding(TB)-Hamiltonian analysis, which is frequently employed in analyzing graphene band-

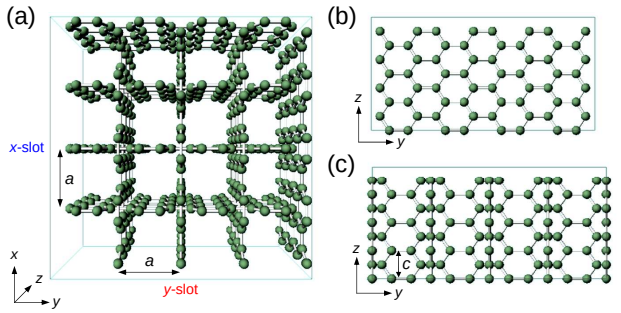

FIG. 1. (a) Hopfene made of horizontally- and vertically-combined graphene sheets where the intersections are comprised of Hopf-links; this Hopfene has an empty slot between neighboring graphene sheets [13, 14]. (b) Graphene sheet before vertical graphene sheets are inserted. (c) Graphene sheet after they are inserted; this insertion swells carbon hexagons in the y (and x) direction.

structures. Later in this paper, those DFT- and TB-analysis results will be compared with each other, particularly to determine transfer-energy parameters for Hopf-links in the TB model.

A difference in Hamiltonian between Hopfenes and graphenes is that since the Hopfenes have Hopf-linked intersections (where graphenes meet), the total Hamiltonian has an extra component $\mathcal{H}_{\rm H}$ concerning electron transfer via the Hopf-links in addition to ordinary graphene transfer Hamiltonians $\mathcal{H}_{\rm G}(h_{\rm AB})$ and $\mathcal{H}_{\rm G}(h_{\rm CD})$ defined in A- and B-sublattices on the x-z plane and C- and D-sublattices on the y-z plane (see Figs. 2(a)(b)). The presence of $\mathcal{H}_{\rm H}$ affects Dirac-point symmetries that graphenes originally have [15]. Note that there is a difference in theory-applicable range between TB and DFT analyses, where TB analysis can deal with perfect hexagons and DFT analysis can *also* deal with deformed hexagons, which is out of reach of TB approach; yet TB approach is sometimes *still* effective in extracting important basic features of electronic bands, which will be shown below.

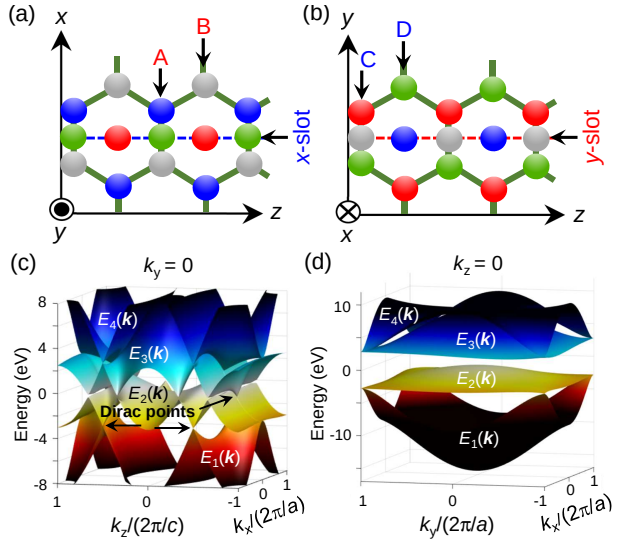

FIG. 2. (a) Graphene sheet parallel to the x-z plane that defines A- and B-sublattices, including Hopf-links, with x-slot insertion. (b) Graphene sheet parallel to the y-z plane that defines C- and D-sublattices, including Hopf-links, with y-slot insertion. (c) Band structure in the k_x, k_z directions, obtained by diagonalizing Eq. (1) with $t_{\rm G} = 2.8$ eV and $t_{\rm H} = 1.0$ eV for $k_y = 0$. Dirac points reflecting those of graphene sheets are observed. (d) Band structure obtained with the same $t_{\rm G}$ and $t_{\rm H}$ in the k_x, k_y directions for $k_z = 0$, which exhibits a flat band.

The total TB Hamiltonian [15] is given by

$$\hat{H} = \sum_{\mathbf{k},\sigma} \sum_{\mu,\nu=1}^{2} \hat{\psi}^{\dagger(\mu)}_{\mathbf{k}\sigma} \mathcal{H}^{\rm total}_{\mu\nu} \hat{\psi}^{(\nu)}_{\mathbf{k}\sigma}, \qquad (1)$$

where $\hat{\psi}^{(1)}_{\mathbf{k}\sigma} = (a_{\mathbf{k}\sigma}, b_{\mathbf{k}\sigma})$ and $\hat{\psi}^{(2)}_{\mathbf{k}\sigma} = (c_{\mathbf{k}\sigma}, d_{\mathbf{k}\sigma})$ are annihilation operators for electrons of momentum $\mathbf{k}$ (in units of $(2\pi/a, 2\pi/a, 2\pi/c)$) and spin σ in A- and B-sublattices and C- and D-sublattices, respectively, which are basically equivalent, except for plane directions; their adjoints $\hat{\psi}^{\dagger(1)}_{\mathbf{k}\sigma}$ and $\hat{\psi}^{\dagger(2)}_{\mathbf{k}\sigma}$ are electron-creation operators; and $\mathcal{H}^{\rm total}_{\mu\nu}$ are defined as $\mathcal{H}^{\rm total}_{11} = \mathcal{H}_{\rm G}(h_{\rm AB})$, $\mathcal{H}^{\rm total}_{22} = \mathcal{H}_{\rm G}(h_{\rm CD})$, $\mathcal{H}^{\rm total}_{12} = \mathcal{H}_{\rm H}$, and $\mathcal{H}^{\rm total}_{21} = \mathcal{H}^{\dagger}_{\rm H}$ (these are all 2×2 matrices). For a (2,2)-Hopfene, $[\mathcal{H}_{\rm G}(h_i)]_{11} = [\mathcal{H}_{\rm G}(h_i)]_{22} = 0$, $[\mathcal{H}_{\rm G}(h_i)]_{12} = [\mathcal{H}_{\rm G}(h_i)]^{*}_{21} = h_i$ (i = AB, CD) with $h_{\rm AB} = -t_{\rm G}(e^{ik_x a/3} + 2e^{-ik_x a/6}\cos(k_z c/2))$, $h_{\rm CD} = -t_{\rm G}(e^{ik_y a/3} + 2e^{-ik_y a/6}\cos(k_z c/2))$, and $\mathcal{H}_{\rm H} = -t_{\rm H}(\phi^{\dagger}_{-k_x/6}\phi_{k_y/3} + \phi^{\dagger}_{k_x/3}\phi_{-k_y/6} + 2\cos(k_z c/2)\phi^{\dagger}_{-k_x/6}\phi_{-k_y/6})$ with $\phi_k = (e^{ika}, e^{-ika})$; here $t_{\rm G}$ and $t_{\rm H}$ are transfer-energy parameters [15]. For $t_{\rm G}$, there is a good reference [5, 20], but for $t_{\rm H}$, there is no such one (and we will obtain this in comparison with the DFT analysis).

If holes are dealt with (when the Fermi level is below a Dirac point), the annihilation and creation operators given above should be switched to those for holes. Moreover, the spin-orbit interaction, which predicts the appearance of 'spin-Hall' effect, is not included in Eq. (1), since we here discuss no such phenomenon as current induction by this effect (and this effect is actually very small in light materials, e.g., carbons, when compared with that in heavy materials, e.g., HgTe-quantum wells).

By diagonalizing Eq. (1) [5, 21] in a numerical manner, we obtain energy-momentum dispersion $E_i(\mathbf{k})$ with band index i, as depicted in Fig. 2(c) in the k_x, k_z directions with $k_y = 0$, where $t_{\rm G}$ is set at 2.8 eV [5, 20] and $t_{\rm H}$ is tentatively set at 1.0 eV. Here we can see some Dirac points reflecting those of graphenes; but the fine detail is different from graphenes: the equivalence of the original six Dirac points is violated by the presence of the Hopf-links, and partially degeneracy-resolved Dirac points appear [15].

A more remarkable difference from the graphenes is the presence of a big flat band, as illustrated in Fig. 2(d) in the k_x, k_y directions with $k_z = 0$; much more flat-band appearances are recognized in a (2,2)-Hopfene with an empty slot between two adjacent graphene sheets (with Schönflies symmetry $\rm P4_2$) than in a (1,1)-Hopfene with a similar structure but a smaller (or minimum, finite) sheet-spacing (with $\rm P4_2bc$) [14].

The flat bands, which provide high density of states (DOS), are useful for improving magnetic and electric properties of crystals, e.g., ferromagnetism [18] and superconductivity [19], where the flat bands much enhance the electron-electron interaction while suppressing one-particle degree of freedom (which is beneficial for such improvement). To make use of those high-DOS flat bands, the level of a flat band should fit the Fermi level. But this is not always satisfied, which actually depends on the band structure and electron filling in a crystal; the flat-band-level tuning is thus necessary. We perform this by carbon-hexagon deformation in the Hopfene.

In addition to Hopfenes, there have been some 3D carbon allotropes proposed so far that show flat bands [23–25]. For effective use of flat-band levels, Fermi-level tuning by means of doping or intercalation is used for the level-fitting; but too much doping for a large Fermi-level shift completely spoils the band structure. Instead, we here describe a flat-band shift by hexagon-deformation while averting this band-structure spoiling due to too much doping, and perform precise level-tuning while keeping the flatness of the band; this enables large level-tuning ($\sim$ eV). This type of research has not fully been performed yet in other 3D carbon allotropes.

We find via DFT analysis that the sheet insertion (which swells the carbon hexagons in the x, y directions) can shift the flat-band level, where we start from perfect hexagons in a (2,2)-Hopfene, and see an effect of gradual hexagon-deformation. Band structures (Kohn-Sham-eigenvalue distributions) of a (2,2)-Hopfene with perfect hexagons are plotted in Fig. 3(a) for TB (colored curves) and DFT results (black circles); their comparison in shape gives qualitatively good agreement (but no exact match), which gives $t_{\rm H} = 1.5$ eV (with a standard deviation of 0.5 eV).

Next, we show the level shift of a flat band, indicated by the black arrow in Fig. 3(a), by deforming the perfect hexagon, starting from the hexagon-deformation rate $\eta = 0$ (%). As seen in Fig. 3(b), the level goes down almost linearly as η (%) increases. In Fig. 3(b), the gradient of the energy shift ΔE (eV) vs η (%) is -0.111 (eV/%), where $\eta = 100\,\% \times (a/a_0 - 1)$ with a swelled c-c-bond length a in the x, y directions and the original c-c-bond length a_0 (= 1.42 Å); this means that a 1-% bond extension moves the flat-band level down by 111 meV. This level-shift rate

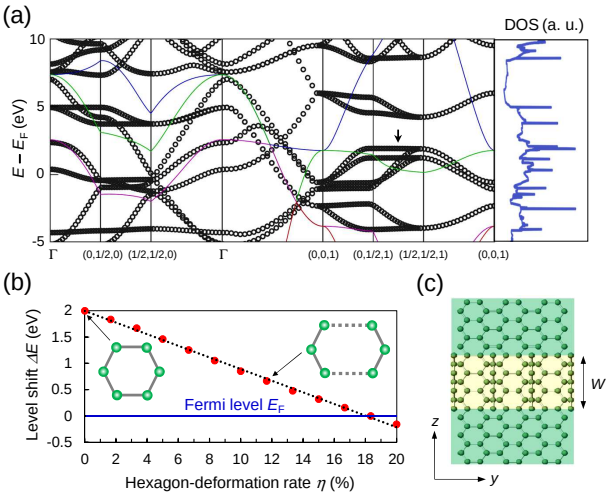

FIG. 3. (a) Band structure of a (2,2)-Hopfene. The black circles come from DFT computations, and thin colored curves come from TB calculations via a fitting of $t_{\rm H}$. (b) Level shift ΔE (eV) of a flat band indicated with the black arrow in (a) depending on the hexagon-deformation rate η (%), where ΔE is measured from the Fermi level $E_{\rm F}$. At $\eta = 18.2$ %, the flat band matches $E_{\rm F}$; such a large c-c-bond extension is known to be allowed for graphenes [22]. (c) Double-hetero-like structure for hexagon-deformation control in the Hopfene (yellow), where the Hopfene is sandwiched between graphene layers (green). Adjusting the size of W controls η.

does not so much differ from that (for holes) produced by strain-induced band-deformation in semiconductors [26]. The level shift for electrons in the semiconductors is small compared with that for holes, particularly for heavy holes, but the electron level shift in our Hopfene is comparable to that heavy-hole level shift, which may be due to dealing with 'heavy' electrons at the flat band produced by large band-deformation.

So far the linear dependence of ΔE on η has not yet been explained well. In addition to the strain effect, there could be interaction effects between electrons at the c-atoms; more specifically, the c-c-bond swelling could decrease the repulsive-interaction energy for electrons localized at the c-atoms in the bonds. Also, we need to take into account other interaction effects, since there are π-electrons distributed extensively in the crystal [14], interacting with each other, and interacting with the localized electrons at the c-atoms and also electrons around σ-bonds. These complicated interaction effects could be associated with the relation between ΔE and η.

As seen in Fig. 3(b), at $\eta = 18.2$ (%) the flat-band level comes across the Fermi level $E_{\rm F}$. Since $\eta \approx 20$ % is kept in natural Hopfenes, those two levels are slightly separated, actually. To control the η-change and stop it at an appropriate η, a pressure application is helpful; but a high pressure on the order of GPa will be necessary. This size of pressure is possible, and a super compressor that generates $\sim$ 100 GPa has actually been developed (to observe superconductivity) [27], but is costly.

We here propose another method that uses a double-hetero(DH)-like structure, as given in Fig. 3(c), which is a similar structure employed for semiconductor strain-band-engineering. With this structure, when the width W is controlled, controlling the hexagon deformation in the y direction is possible. If W is small, or comparable to the Hopfene unit-cell size, the Hopfene hexagons are almost undeformed, i.e., almost the same as those of graphenes placed at both sides of the Hopfene. As W increases, the deformation becomes large. Detailed calculations for appropriate W will be necessary for those levels to fit exactly. Here we should note that in our proposed DH-like structure, deformation controls both in the x, y directions are not performed simultaneously; in Fig. 3(c), it controls only the flat-band level in the y direction. Controlling the level in the x direction is possible by switching y to x in directions (but with no simultaneous controls in the x, y directions). This limits an available k-space in flat-band modulation, but does not destroy a level-shifting way reported in this paper.

In summary, we have examined the band structures of Hopf-linked graphene crystal named Hopfene via TB and DFT analyses. We have seen that they agree qualitatively well with each other via TB-parameter fitting. The hexagon deformation on a flat-band-level shift in a (2,2)-Hopfene has been analyzed by the DFT method, which cannot be easily made by the TB method including free parameters. That deformation enables fitting the flat band to the Fermi level (where its large DOS will be used for magnetic and electric researches [18, 19]). With an increase in the hexagon-deformation rate η, we have observed a linear lowering of the flat-band level, where the flat band meets the Fermi level at a certain η. We also have put forward an idea using a DH-like structure to control η and the flat-band level, without applying a very high pressure.

ACKNOWLEDGMENT

This work is supported by EPSRC Manufacturing Fellowship (EP/M008975/1). I.T. would like to thank ECS at University of Southampton, where the idea of the present research was come up with. (The data of the paper can be obtained from the University of Southampton ePrint research repository: https://doi.org/10.5258/SOTON/D0953.) We would also like to thank JAIST for its hospitalities during our stay at the Center for Single Nanoscale Innovative Devices. Thanks are also due to Prof. H. Mizuta, Dr. M. Muruganathan, Prof. Y. Oshima, Prof. S. Matsui, Prof. S. Ogawa, Prof. S. Kurihara, and Prof. H. N. Rutt for stimulating and fruitful discussions.

* i.tomita@soton.ac.uk

[1] H. W. Kroto, J. R. Heath, S. C. O'Brien, R. F. Curl, and R. E. Smalley, Nature **318**, 162 (1985).
[2] S. Iijima, Nature **354**, 56 (1991).
[3] K. S. Novoselov, A. K. Geim, S. V. Morozov, D. Jiang, Y. Zhang, S. V. Dubonos, I. V. Grigorieva, and A. A. Firsov, Science **306**, 666 (2004).
[4] S. Iijima, *Challenges of Carbon Nanotunbes* (Iwanami Sci. Lib., Tokyo, 1999).

[5] T. Ando, J. Phys. Soc. Jpn. **74**, 777 (2005).

[6] A. C. Ferrari, J. C. Meyer, V. Scardaci, C. Casiraghi, M. Lazzeri, F. Mauri, S. Piscanec, D. Jiang, K. S. Novoselov, S. Roth, and A. K. Geim, Phys. Rev. Lett. **97**, 187401 (2006).

[7] N. Yoshikawa, T. Tamaya, and K. Tanaka, Science **356** 736 (2017).

[8] M. Bockrath, D. H. Cobden, J. Lu, A. G. Rinzler, R. E. Smalley, L. Balents, and P. L. McEuen, Nature **397**, 598 (1999).

[9] A. F. Hebard, M. J. Rosseinsky, R. C. Haddon, D. W. Murphy, S. H. Glarum, T. T. M. Palstra, A. P. Ramirez, and A. R. Kortan, Nature **350**, 600 (1991).

[10] K. S. Novoselov, A. K. Geim, S. V. Morozov, D. Jiang, M. I. Katsnelson, I. V. Grigorieva, S. V. Dubonos, and A. A. Firsov, Nature **438**, 197 (2005).

[11] K. Nomura, S. Ryu, and D. H. Lee, Phys. Rev. Lett. **103**, 216801 (2009).

[12] J. P. Sauvage, Angew. Chem. Int. Ed. **56** 11080 (2017).

[13] S. Saito and I. Tomita, arXiv:1904.08107.

[14] I. Tomita and S. Saito, Solid State Comm. (2019) submitted.

[15] S. Saito and I. Tomita, arXiv:1904.12784v2.

[16] P. Giannozzi *et al.*, J.Phys.: Cond. Matt. **21**, 395502 (2009).

[17] P. Giannozzi *et al.*, J.Phys.: Cond. Matt. **29**, 465901 (2017).

[18] E. H. Lieb, Phys. Rev. Lett. **62**, 1201 (1989).

[19] R. Mondaini, G. G. Batrouni, and B. Gremaud Phys. Rev. B **98**, 155142 (2018).

[20] A. H. Castro Neto, F. Guinea, N. M. R. Peres, K. S. Novoselov, and A. K. Geim, Rev. Mod. Phys. **81**, 109 (2009).

[21] A. Suzuki, M. Tanabe, and S. Fujita, J. Mod. Phys. **8**, 607 (2017).

[22] S. Sorella, K. Seki, O. O. Brovko, T. Shirakawa, S. Miyakoshi, S. Yunoki, and E. Tosatti, Phys. Rev. Lett. **121**, 066402 (2018).

[23] T. Kiryu and M. Koshino, Phys. Rev. B **99**, 085443 (2019).

[24] C. Zhong, Y. Chen, Y. Xie, S. A. Yang, M. L. Cohenc, and S. B. Zhang, Nanoscale **13**, 7232 (2016).

[25] J. Hua, W. Wua, C. Zhong, N. Liu, C. Ouyang, H. Y. Yanga, and S. A. Yang, Carbon **141**, 417 (2019).

[26] S. Seki, T. Yamanaka, W. Lui, Y. Yoshikuni, and K. Yokoyama, IEEE J. Quantum. Elec. **30**, 500 (1994).

[27] A. P. Drozdov, P. P. Kong, V. S. Minkov, S. P. Besedin, M. A. Kuzovnikov, S. Mozaffari, L. Balicas, F. F. Balakirev, D. E. Graf, V. B. Prakapenka, E. Greenberg, D. A. Knyazev, M. Tkacz, and M. I. Eremets, Nature **569**, 528 (2019).